

## **General Disclaimer**

### **One or more of the Following Statements may affect this Document**

- This document has been reproduced from the best copy furnished by the organizational source. It is being released in the interest of making available as much information as possible.
- This document may contain data, which exceeds the sheet parameters. It was furnished in this condition by the organizational source and is the best copy available.
- This document may contain tone-on-tone or color graphs, charts and/or pictures, which have been reproduced in black and white.
- This document is paginated as submitted by the original source.
- Portions of this document are not fully legible due to the historical nature of some of the material. However, it is the best reproduction available from the original submission.

Final Report

NASA DART Grant No. NAS6-2826

(NASA-CR-141436) NASA DART Final Report  
(Pennsylvania State Univ.) 27 p  
HC A03/MF A01

N78-20165

CSCS 22E

G3/15      Unclass  
11834

National Aeronautics and Space Administration

Wallops Island, Virginia 23337

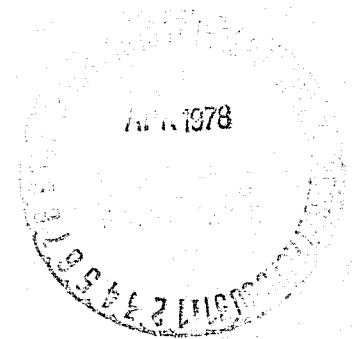
Submitted by

Leslie C. Hale, Principal Investigator

Ionosphere Research Laboratory

The Pennsylvania State University

August 26, 1977



## CHAPTER I

## INTRODUCTION

The blunt probe has evolved slowly over a ten-year period to become a fairly routine electrical conductivity measurement system. Originally developed for the Super Arcas sounding rocket,<sup>1</sup> it has undergone several refinements while maintaining a basic compatibility with the meteorological sounding range support system. Historically, data from the mesosphere was of prime interest, but with increased sensitivity, conductivities extending into the stratosphere are possible.

The positive and negative conductivities produced by this technique have been studied for insights into the dependence of the stratosphere and mesosphere on various geophysical influences.<sup>2</sup> Once the basic theory of ion collection was developed<sup>3,4</sup> and verified experimentally, various specific programs have yielded much information. Early work showed that nighttime ionization in the 45 to 75 km region at mid-latitudes follows a simple model.<sup>5</sup> Daytime results have shown that the transition region from solar to cosmic ray ionization (normally at 63.5 km) can be related to the density of nitric oxide, the main ion constituent in this region.<sup>6</sup> When a large enough statistical base was assembled, several interesting correlations were observed. Daytime negative conductivity in the 50 to 60 km region correlates well with radio wave absorption which occurs at high altitudes. Positive ion conductivity correlates well with the neutral atmosphere temperature between 33 and 58 km. The temperature coefficient observed is larger than that predicted by a simple ion chemistry model.<sup>7</sup>

In 1968 a direct NO measurement was made by observing the change in conductivity produced by an in situ ultraviolet lamp to photo-ionize NO.<sup>8</sup> Recently this work has continued with a larger sounding rocket payload utilizing a different probe geometry.<sup>9</sup>

Data obtained during the "winter anomaly," when increased radio wave absorption is observed, have shown an enhancement of positive conductivity when compared to "normal" days.<sup>10</sup>

Not all experiments can be defined with a few launches, however. Some observations require a statistical base to demonstrate a predicted relationship. The use of the Super Loki Dart sounding rocket is attractive for reducing flight costs and simplifying payload production. A Super Loki blunt probe system has been developed with plans and blueprints with several concurrent test firings. Now these probes can be produced either in-house or commercially. It is expected that greater flexibility in planning specific programs will result, with a larger catalog of data accumulating for statistical analysis.

## CHAPTER II

## THE BLUNT PROBE EXPERIMENT

The basic operation of the blunt probe has been described elsewhere,<sup>11,12</sup> but will be briefly repeated here. The blunt probe is most useful as a subsonic probe, deployed on a parachute, with data telemetried back to the ground station via an L-band transmitter. A known waveform is applied between two electrodes immersed in the surrounding plasma and the resultant current is observed. By use of the appropriate geometric scale factors, one can then compute the ion conductivity.

As illustrated in Figure 2.1, the probe hangs vertically beneath a parachute. A large return electrode covers most of the long cylindrical section, while the front plate consists of a circular collector disk surrounded by a guard ring. This guard ring is maintained at the same potential as the collector disk and controls the fringing electric fields so that the E field at the collector disk is uniform and predictable. The current flowing to the collector disk is measured by an electrometer.

The sweep waveform of Figure 2.2 is applied to the return electrode. When this sweep waveform is positive, positive ions are collected at the collector; when the sweep is negative, negative particles are collected. As the applied sweep voltage is changed linearly, one observes the collector current also changes linearly, as predicted. Both negative ions and electrons (if present) are collected when the sweep is negative. Due to the high electron conductivity, the observed V-I characteristic usually has a different slope for negative sweeps.

In one sense, the observed V-I characteristic is a measure of the conductance of the electrodes with the plasma. One must reduce any effects between the return electrode and the medium. The large size

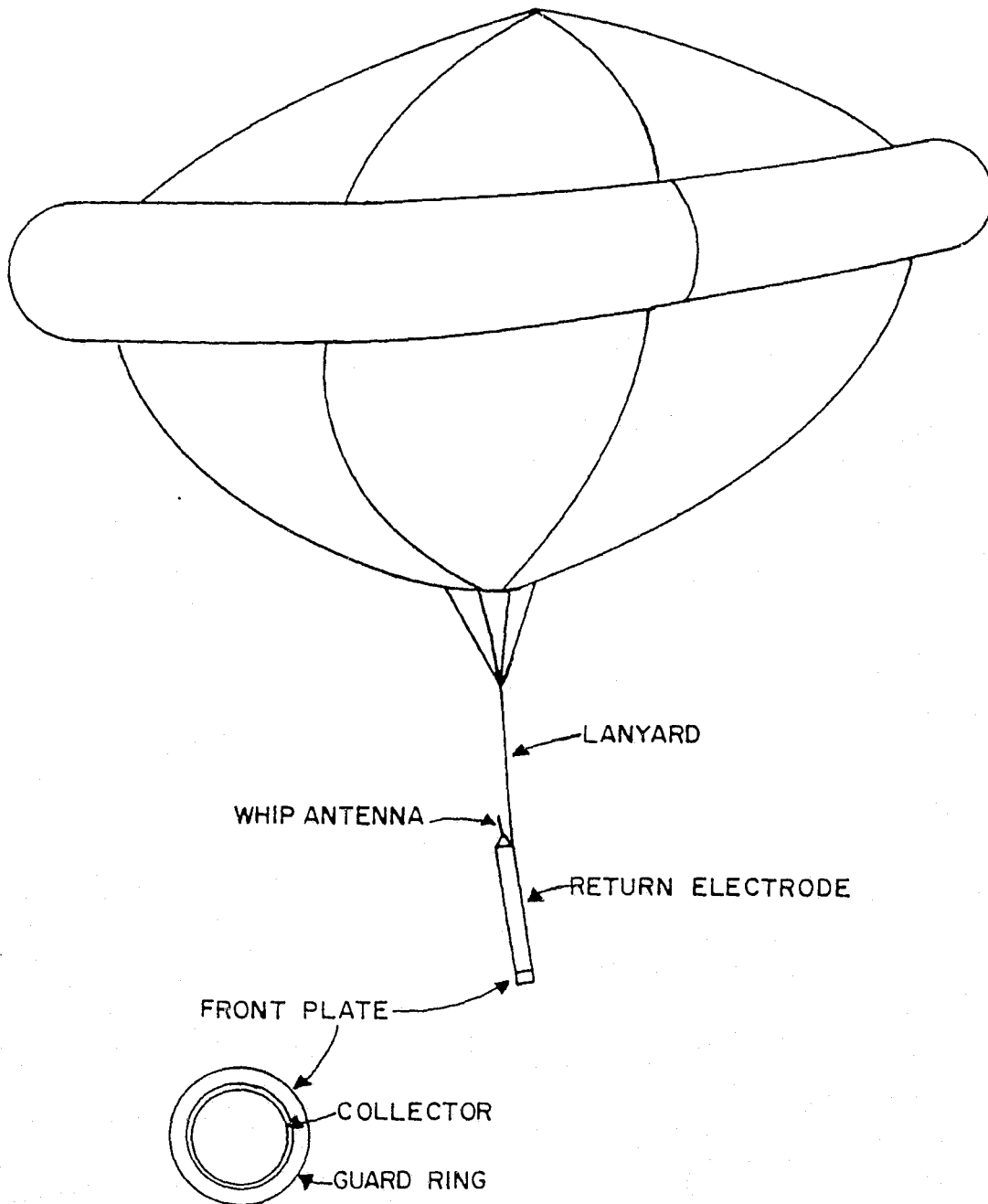


Figure 2.1: Deployed Super Loki Dart blunt probe.

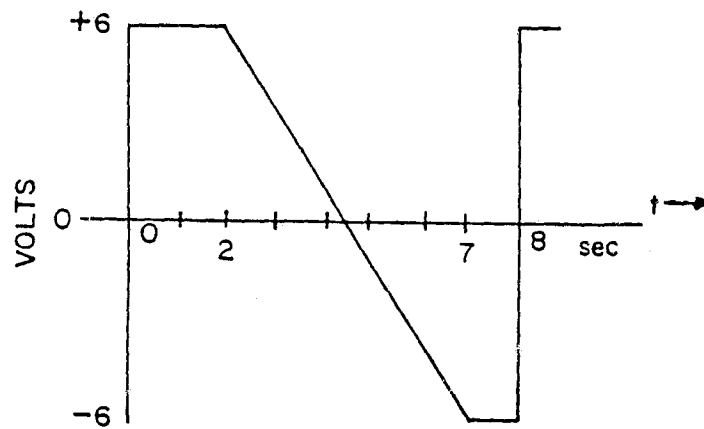


Figure 2.2: Sweep waveform applied between electrodes.

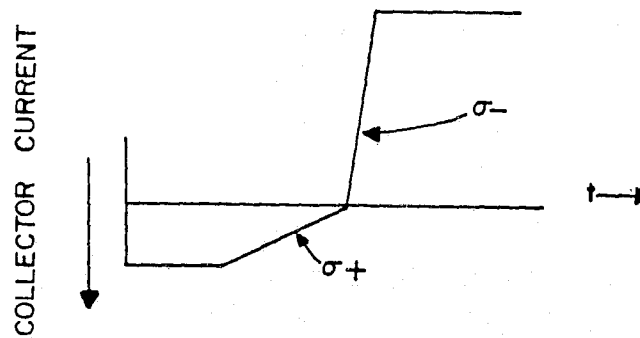


Figure 2.3: Typical observed current waveform.

of the return electrode helps, but at night the solution is not explicit so that an iterative data reduction procedure is necessary.<sup>13</sup>

In the daytime, however, the situation is improved by photo emission from the sides of the payload produced by the sun. This large electron photo emission forces the payload slightly positive a few tenths of a volt until enough highly mobile electrons are attracted to produce an equilibrium. The result is that a relatively low impedance "connection" is maintained between the return electrode and the plasma. The "contact potential" of a few tenths of a volt varies with altitude and payload profile presented to the sun. Unstable parachutes sometime result in a modulation of this profile and potential and the collected electron current. With the return electrode thus essentially held at the plasma potential, the front collector is swept both positively and negatively. The downward facing front plate avoids photo emission from the surface. Solar zenith angles may be important if large parachute swings are expected.

A typical data waveform is shown in Fig. 2.3. Here the positive conductivity observed first is less than the negative conductivity. A large dynamic range ( $10^3$  to  $10^4$ ) can be handled in this way since the slope can vary from very steep to very flat and still be observable by appropriate expansion of the vertical or horizontal time scale during data tape playback.

Payload calibration is performed as a ground preflight procedure. Since the conductivity of the atmosphere at sea level is very low, the observed payload response is very small, essentially no vertical deflection. A minute or so of data recorded in this "flight" mode provides a permanent indication of payload health. Then a calibration is recorded for a few



minutes by engaging a relay which switches in a known high value resistor between the sweep and the collector. During data playback, the calibration section of data is reproduced for each setting of the chart recorder sensitivity and speed. In this way all intermediate systematic errors are removed.

Manual data reduction consists of finding the slopes of each conductance and relating these slopes to the corresponding  $\sigma_+$  or  $\sigma_-$  through a payload geometry factor. The time code which has been recorded on a separate tape channel is used with radar data to determine the altitude of the probe at each sweep time. The real time data chart from the TMQ-5 recorder of the GMD L-band receiver is useful for planning the data reduction of a particular flight. Usually three or four different expansion factors are needed. A full scale (0 to 200 Hz) playback at a fast chart speed (20 mm/sec) is needed for the large conductivities observed directly after expulsion. Since the negative conductivities are very large, a fast response chart recorder is required (BW  $\approx$  100 Hz). A second data playback with an expanded vertical scale and a slower chart speed (5 mm/sec) is used. Later portions of the flight may require an even larger (10 or 20 Hz) vertical expansion. For each chart record, a calibration record is also made with the same recorder settings. The average of the calibration slopes is used in the computation of the conductivities.

Data reduction proceeds by finding the slope of each part of each sweep and then computing the corresponding conductivity by use of the proper probe theory.

$$\sigma_+ = \frac{R}{2r^2 R_{cal}} \frac{\text{data slope}}{\text{data slope}_{avg}} + \text{mho/cm} \quad (1)$$

$$\sigma_- = \frac{R}{2r^2 R_{cal}} \frac{\text{data slope}}{\text{cal slope}_{avg}} - \text{mho/cm} \quad (2)$$

where for the Super Loki blunt probe,  $r$  is the radius of the collector disk, .5 inch;  $R$  is the radius of the guard ring, 13/16 inch; and  $R_{cal}$  is the resistance of the calibration resistor.

Thus converting the dimensions to metric,

$$\sigma_{\pm} = \frac{.6476}{R_{cal}} \frac{\text{data slope} | \pm}{\text{cal slope} | \text{avg}} \text{ mho/cm} \quad (3)$$

## CHAPTER III

## SUPER LOKI BLUNT PROBE

A block diagram of the blunt probe is shown in Figure 3.1. A six volt nickel cadmium battery supplies power to the transmitter tube filament and a power supply converter which in turn produces +110 volts for the transmitter and  $\pm 7.5$  volts, regulated, for the rest of the electronics. A sweep generator produces the desired sweep waveform which is applied to the return electrode. The current received by the collector is measured by an electrometer whose output voltage drives a voltage-controlled oscillator. This VCO has a linear modulation characteristic with a nominal 100 Hz center frequency.

$$f_{\text{out}} = (100 - K I_{\text{collector}}) \text{Hz} \quad (4)$$

for a zero to 200 Hz span. The short negative pulses from the VCO momentarily turn off the L-band transmitter at the repetition rate of the VCO.

The complete schematic of the blunt probe is shown in Fig. 3.2. Internal power is activated by a latching relay, RY1. Short energizing pulses through the umbilical engage or disengage this relay. Operation on external power through the umbilical is also possible. This control arrangement is identical to that of the Loki datasonde system. The power supply inverter is similar to that used in the Super Loki Transponder Datasonde,<sup>15</sup> except that symmetric low voltage supplies are used.

The sweep generator is formed by three sections of the LM324 quad operational amplifier. The first section is a free running multivibrator which determines the basic sweep rate and "rest" period at the beginning of each sweep. Sweep capacitor C6 is charged through diode D4. This

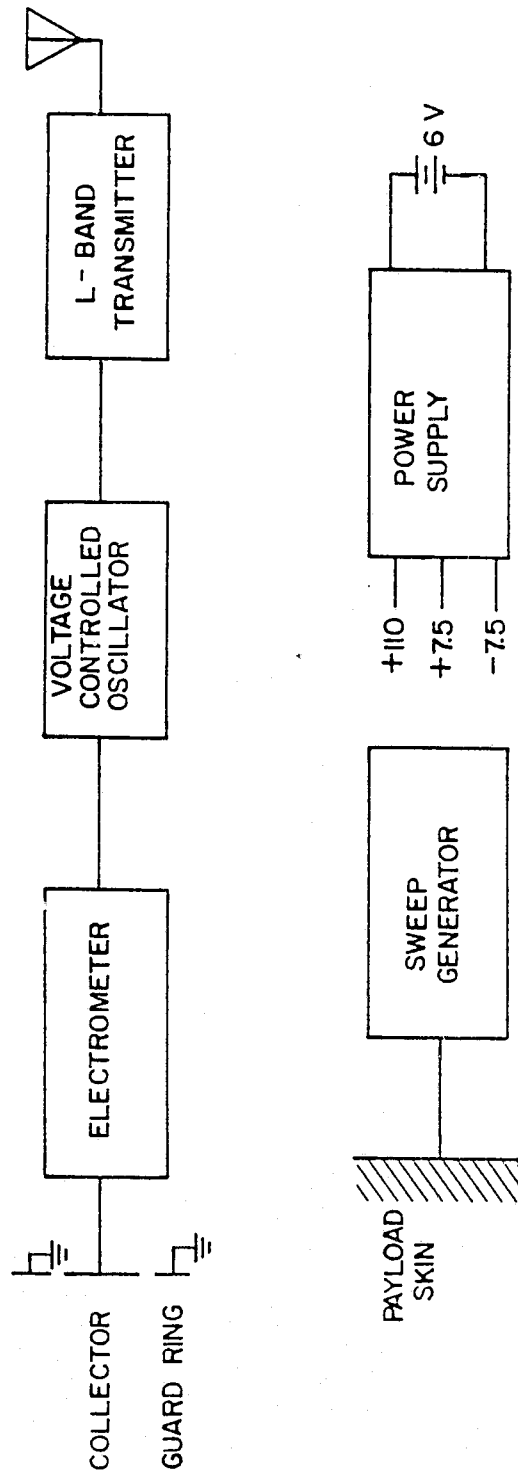


Figure 3,1: Blunt probe block diagram.

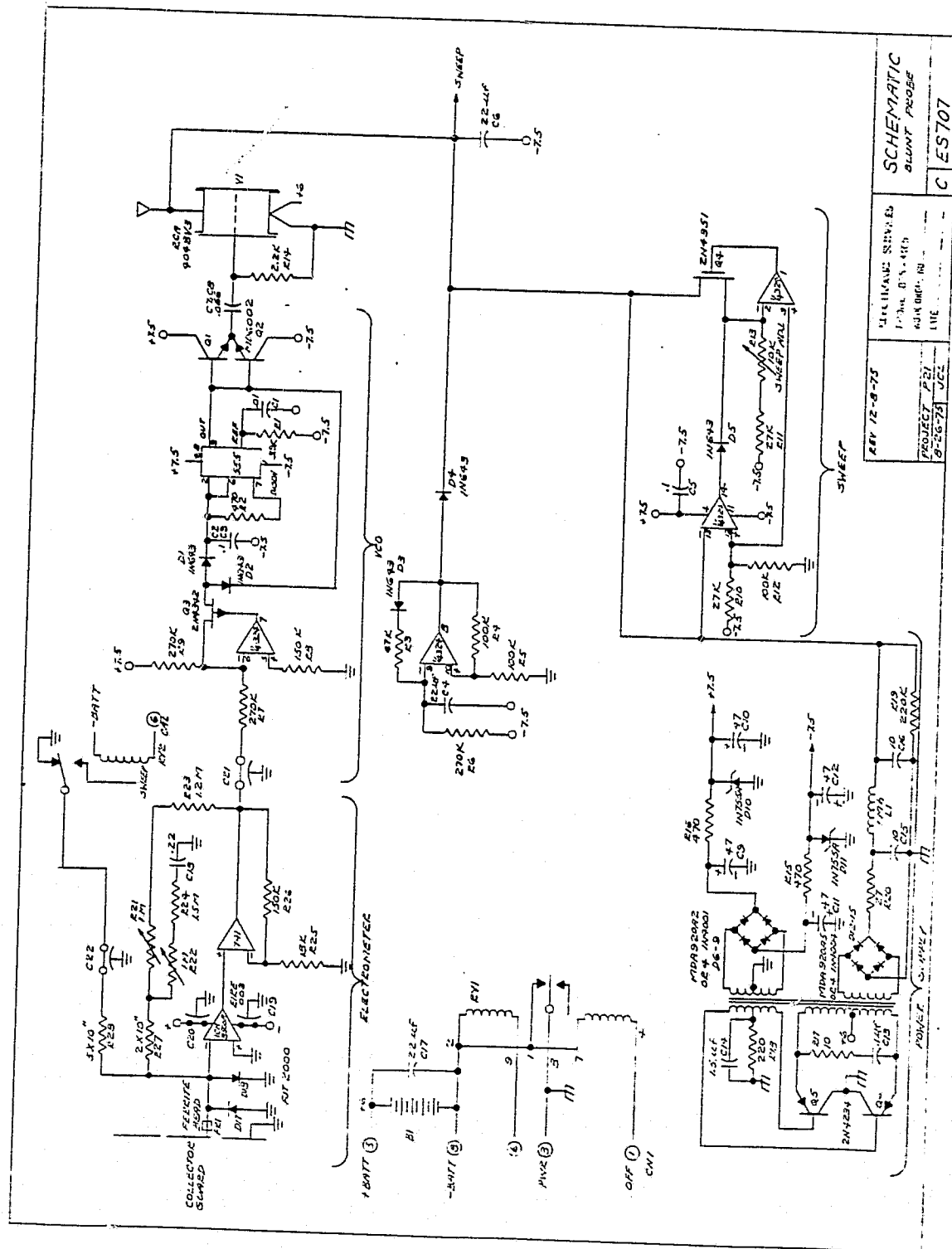


Figure 3.2: Super Loki blunt probe schematic.

ORIGINAL PAGE IS  
OF POOR QUALITY

capacitor is then linearly discharged by a constant current sink formed by  $Q_4$  and another op amp section. The third section is used as a comparator to turn off the current sink at the end of the desired sweep.

The electrometer is made possible by the very small input bias current required by the ICH 8500A. This MOSFET input operational amplifier converts the collector current to an output voltage. The sensitivity is determined by feedback resistor R27. The negative feedback action maintains the collector disk at the guard potential. A resistor-capacitor network consisting of R21, R22, R23, R24, and  $C_{18}$  provide frequency compensation for the best response time of the electrometer. The 741 op amp increases the loop gain for increased response time but is not needed for lower sensitivities. The calibration resistor, R28, is switched between ground for "flight" mode and the sweep output ("cal.") by relay RY2. The entire electrometer is contained within a shielded assembly to prevent RF interference.

The VCO uses the last section of the quad op amp to generate a current proportional to the electrometer output.  $C_2$ ,  $C_3$  are the VCO timing capacitors while R2 sets the VCO pulse width. These VCO pulses key off the 1680 MHz transmitter which is the same telemetry system used by the Loki datasondes. Final transmitter frequency is field adjustable with a set screw adjustment.

Self-sticking copper foil wrapped around the payload forms the return electrode and is soldered to the conical ground plane for the whip antenna. The one-inch section of exposed fiberglass body next to the guard ring is painted white to reduce the heat gain when exposed to sunlight.

With the lanyard fastened off axis as shown in Fig. 3.3., the probe face is not perpendicular to the airflow, but this particular probe geometry is not sensitive to the angle of attack of the probe. It should also be noted that the umbilical connector at the side of the probe has -110 volts exposed on it which, if left uncovered, will distort the particle collection. Two types of covers have been used. One solution is a small steel spring umbilical flap which closes over the connector. Another solution developed by Space Data Corporation is a small sliding door which retracts under the copper foil return electrode. After the umbilical is pulled, a short pull string guides the cover in place.

All payload surfaces are carefully cleaned with acetone during assembly before the payload is inserted in its staves in the Super Loki Dart body.

Data reduction is accomplished by a tape playback into a tachometer which yields an output voltage proportional to the input frequency (Fig. 3.4). The tachometer consists of a monostable multivibrator which produces uniform height and width pulses which are fed to a lowpass filter. A 10 Hz lowpass rolloff is usually sufficient, but additional filtering may be necessary for noisy data at the expense of reduced response time for high conductivities.

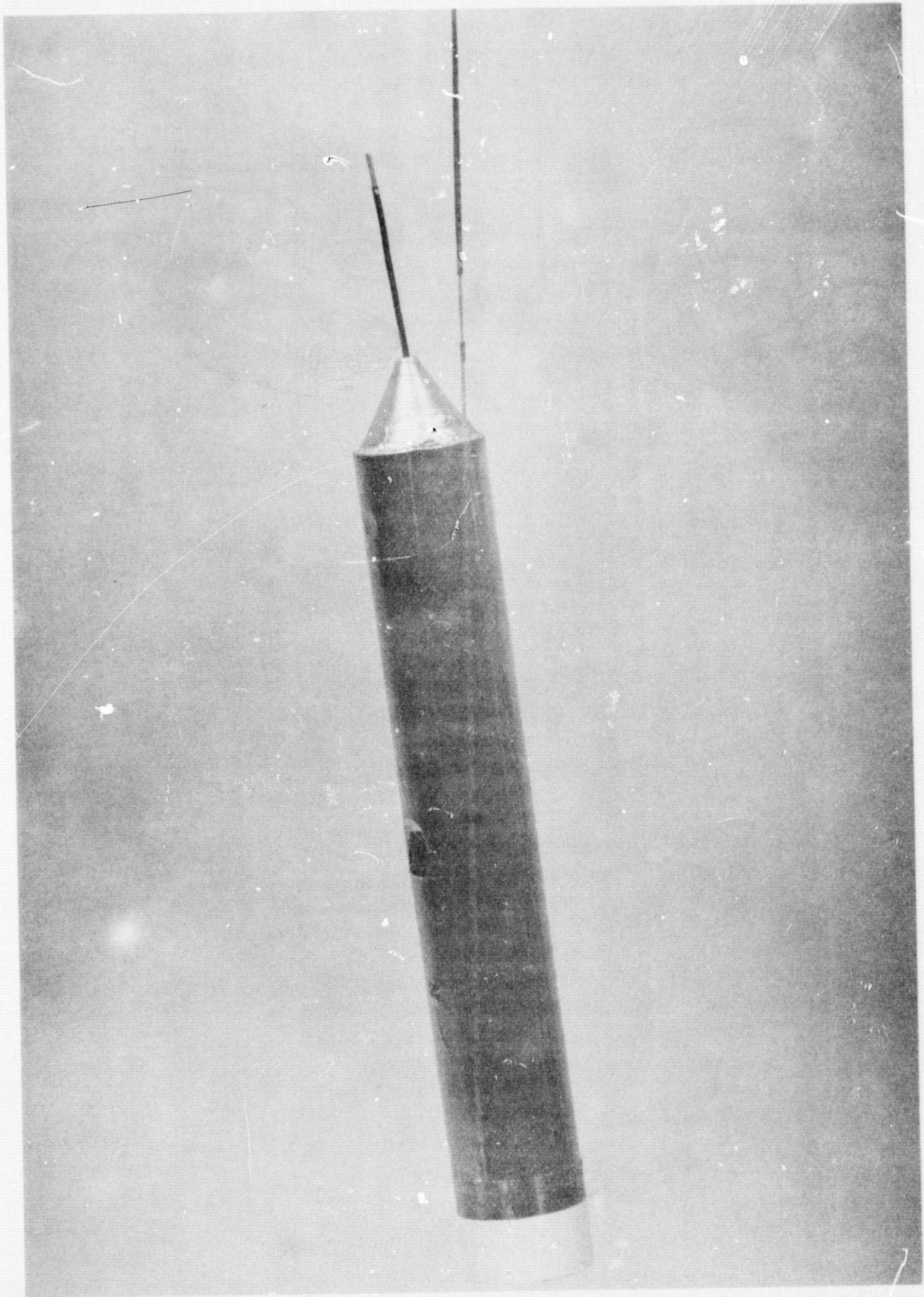


Figure 3.3: Completed Super Loki Dart blunt probe

ORIGINAL PAGE IS  
OF POOR QUALITY



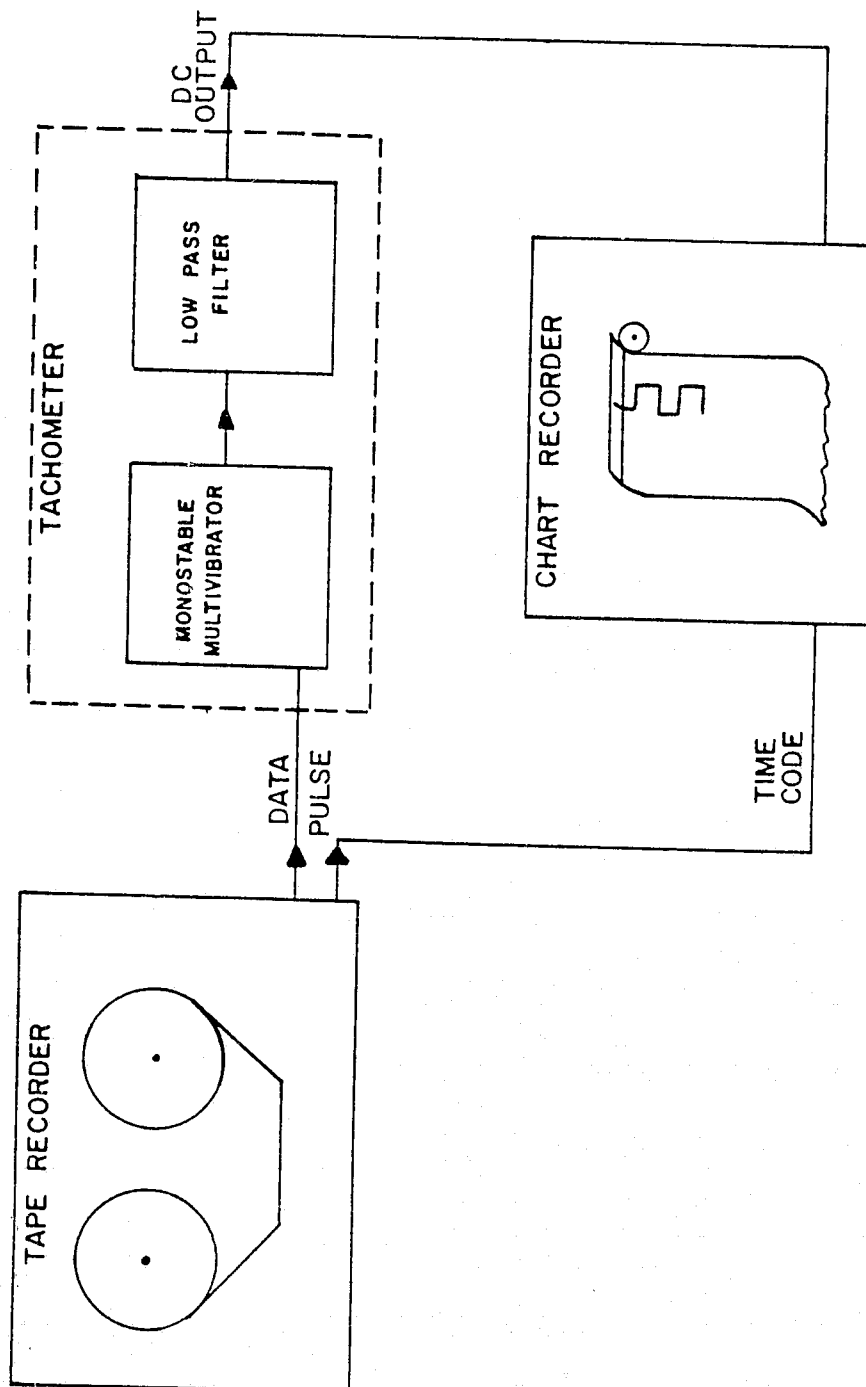


Figure 3.4: Data playback configuration.

## CHAPTER IV

## FLIGHT HISTORY

A series of developmental shots have been used to prove out the design. The first launch on May 2, 1975, was done without an umbilical flap to verify if a flap was indeed necessary. The data obtained (Fig. 4.1) shows nominal positive conductivities, but the negative conductivities are quite depressed, and not unexpected effect on the highly mobile electrons. All later flights have included an umbilical flap (and of course, a cover over the transmitter frequency adjust set screw). While the next payloads were assembled, a detailed assembly manual was written to supplement a complete set of blueprints. One of these flights (Fig. 4.2) experienced a shift in telemetried response causing loss of a portion of the data. A post mortem of the payload after recovery showed that the calibrate relay had not returned to its normally closed ground connection. Since the relay load is a very "dry" circuit, this is a potential problem, but no additional cases have occurred (Fig. 4.3). Eventually a field effect transistor switching network may be necessary. A fourth flight (Fig. 4.4) provided conductivity information as part of the "winter anomaly" campaign at Wallops Island, Virginia, in January 1976. The Dart tail fuse did not function on a fifth launch during the same campaign.

Several production lots have since been constructed from the blueprints and plans both in house at Wallops Flight Center and commercially by Space Data Corporation. That data will be reported elsewhere.

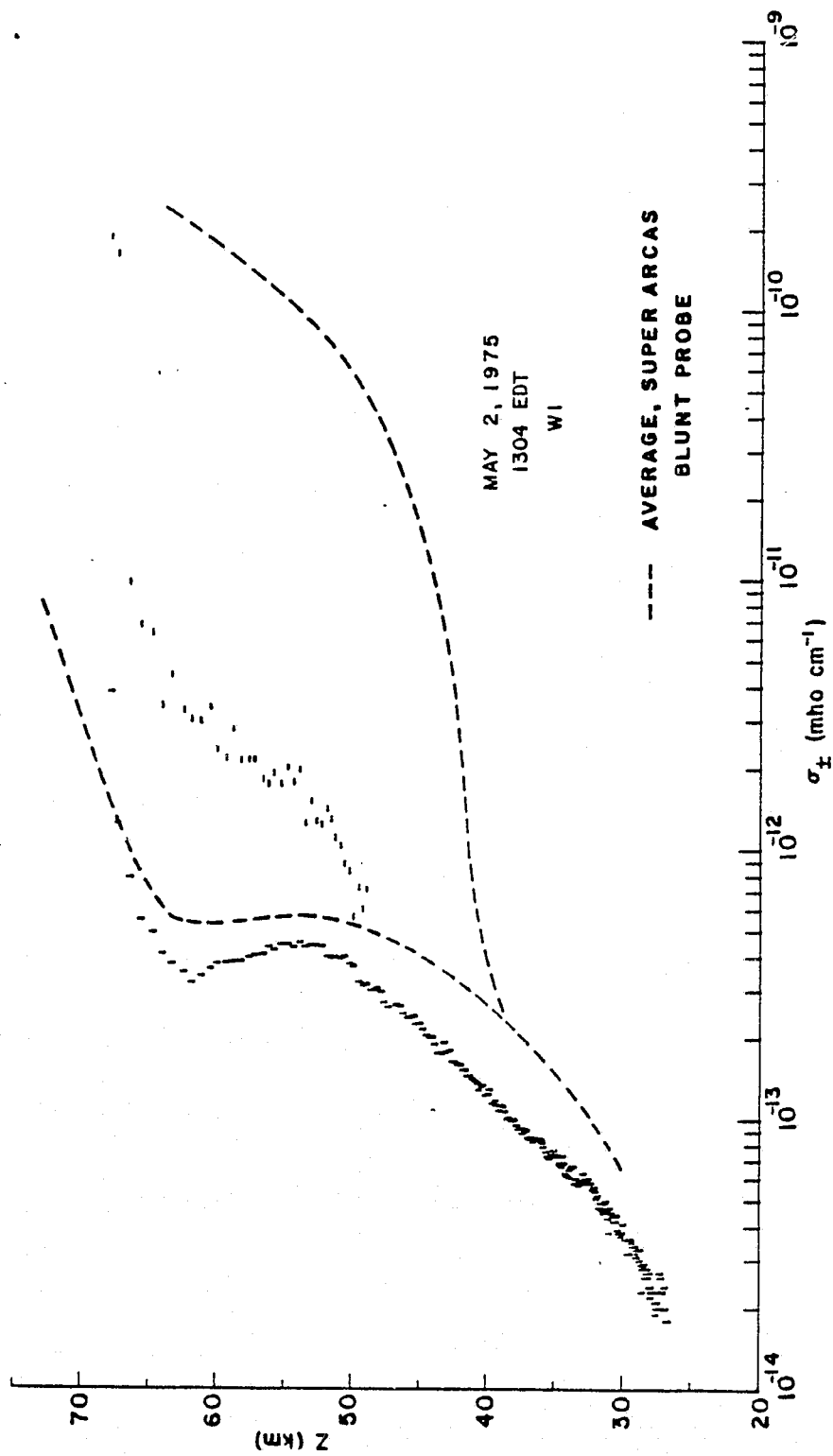


Figure 4.1: Observed conductivities for May 2, 1975.

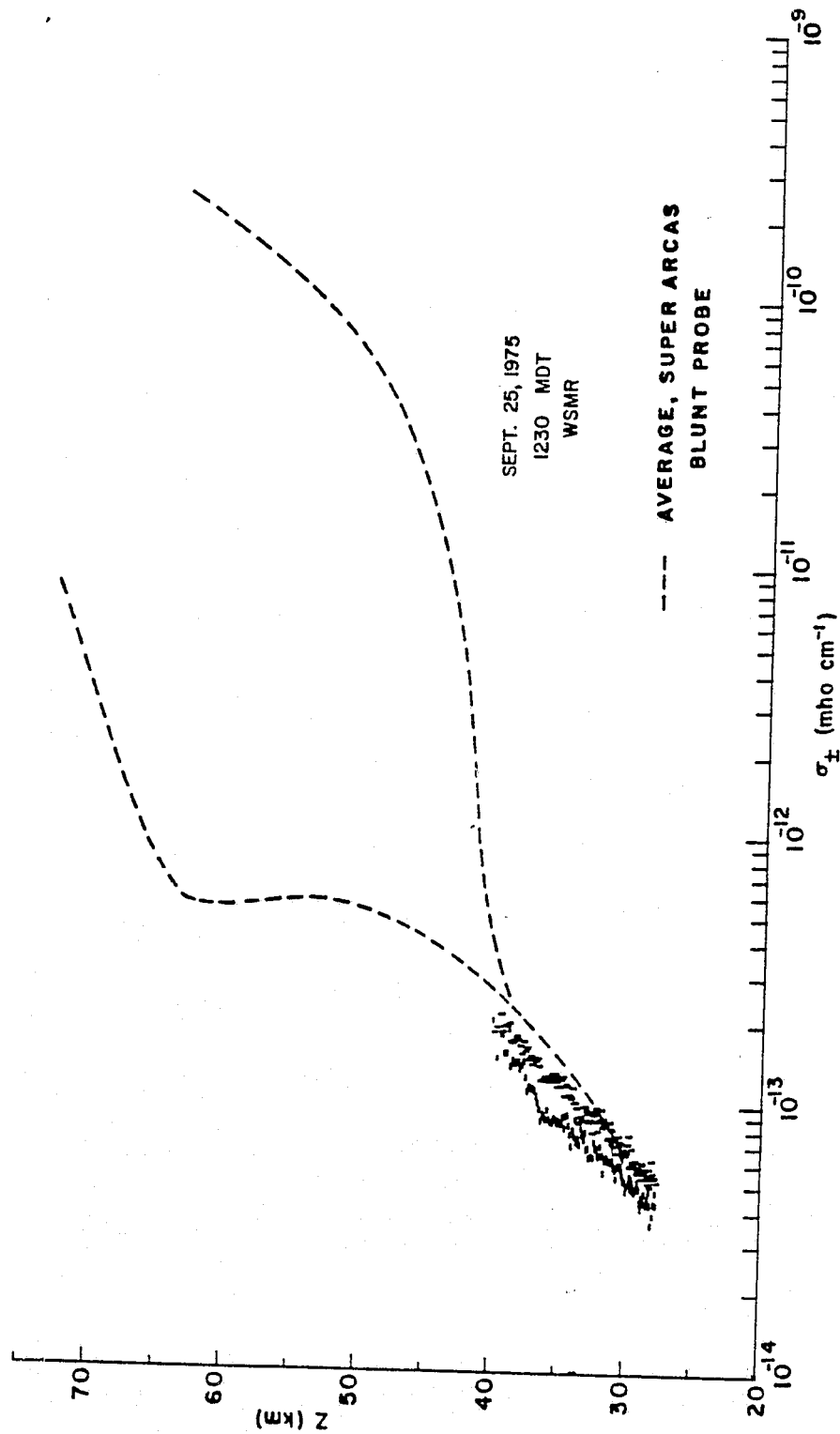


Figure 4.2: Observed conductivities for September 25, 1975.

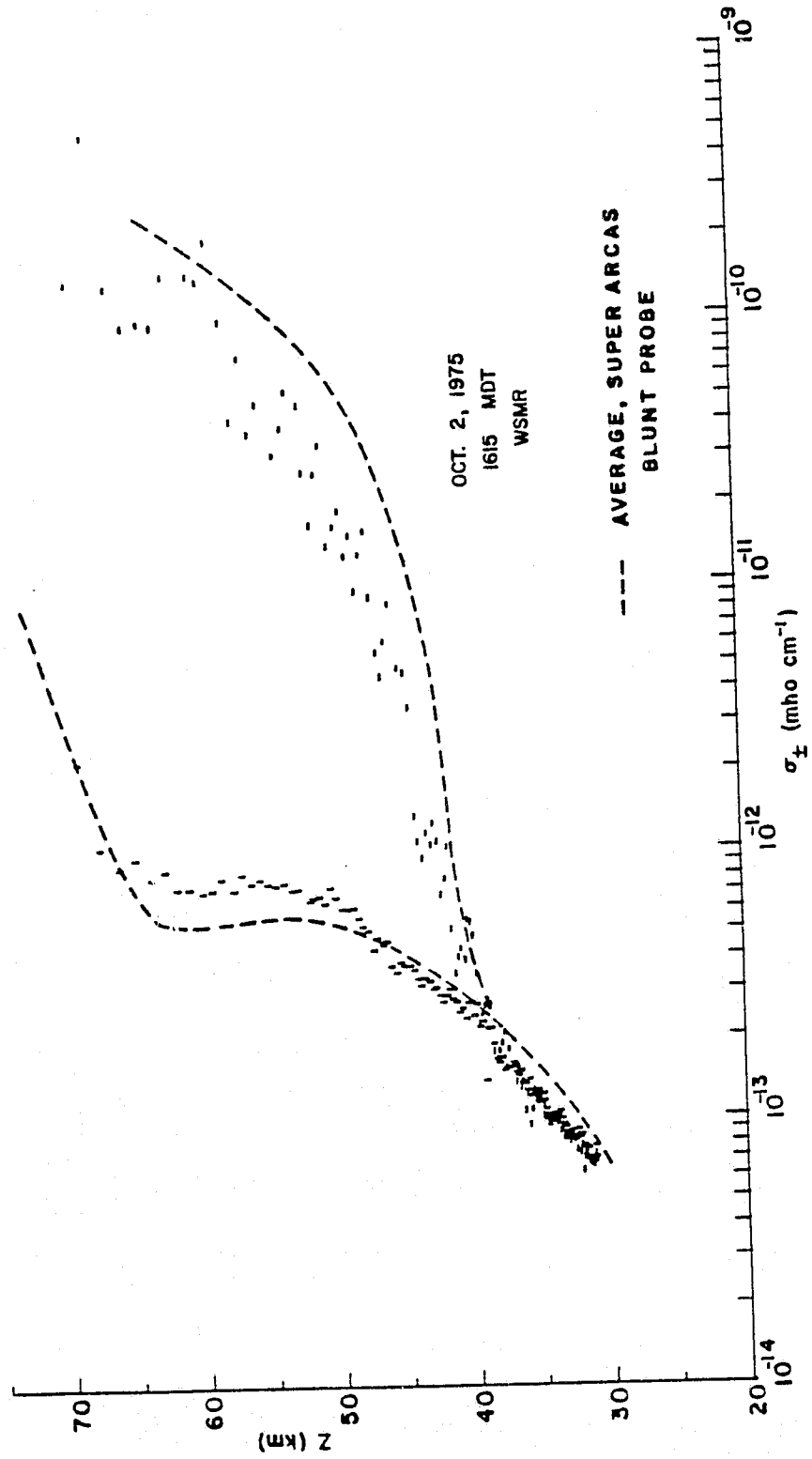


Figure 4.3: Observed conductivities for October 2, 1975.

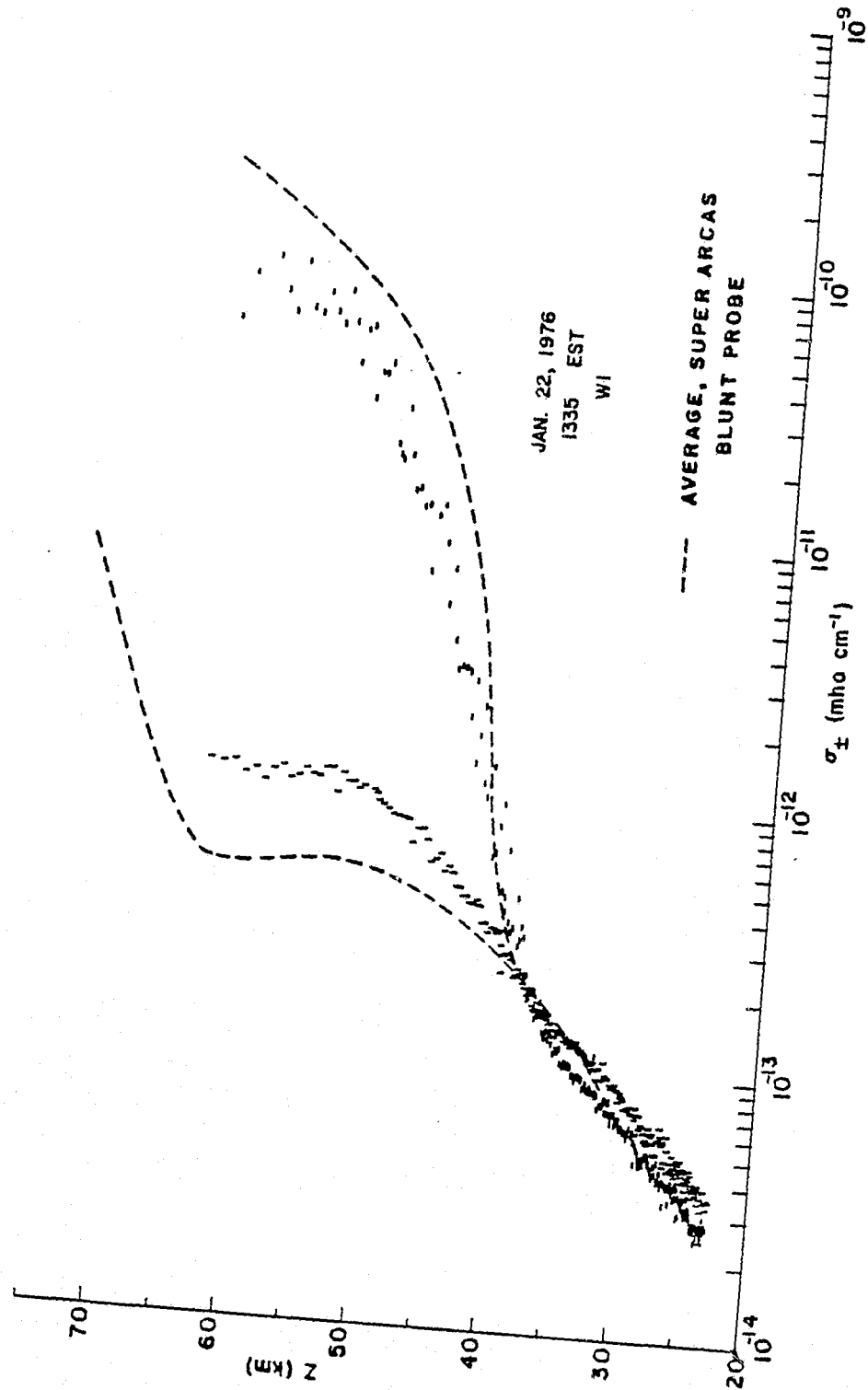


Figure 4.4: Observed conductivities for January 22, 1976.

## CHAPTER V

### IN SITU UV ENHANCEMENTS

The early work of Pontano and Hale<sup>16</sup> in 1968 utilized a Lyman- $\alpha$  (Krypton discharge) ultraviolet lamp with a modified blunt probe for the measurement of nitric oxide. It is expected that NO is selectively ionized by this radiation and the increase in ionization can be compared to the unperturbed medium on alternate sweep cycles. Recently, the technique has been used on Astrobe-D sounding rockets with a Gerdien condenser probe geometry.<sup>15,16</sup> The Gerdien geometry yields more information than the blunt probe, both conductivity and mobility of the ion species; however, it is angle-of-attack sensitive, so that much more stable parachutes are necessary.

An attempt has been made to reduce this payload's complexity and size so that a more synoptic type instrument would result. The Arcas-sized payload of Fig. 5.1 resulted as a development. The size has been reduced to an acceptable level for the Arcas, but the weight is still larger than desired, primarily due to the additional batteries needed to power the UV lamp. A complete schematic is shown in Fig. 5.2. As can be seen, the electrometer telemetry and sweep are similar to that of the blunt probe. In addition, a flipflop counts the sweeps and turns on the VHF lamp oscillator on alternate cycles. Also, the power supply inverter has been modified to better take advantage of available amp-hour capacity.

This particular flight was considered an intermediate design both of hardware and overall experiment. The primary electronic problem remaining is the excessive weight of the lamp batteries. The convenience of rechargeable batteries may have to be foregone for a higher energy

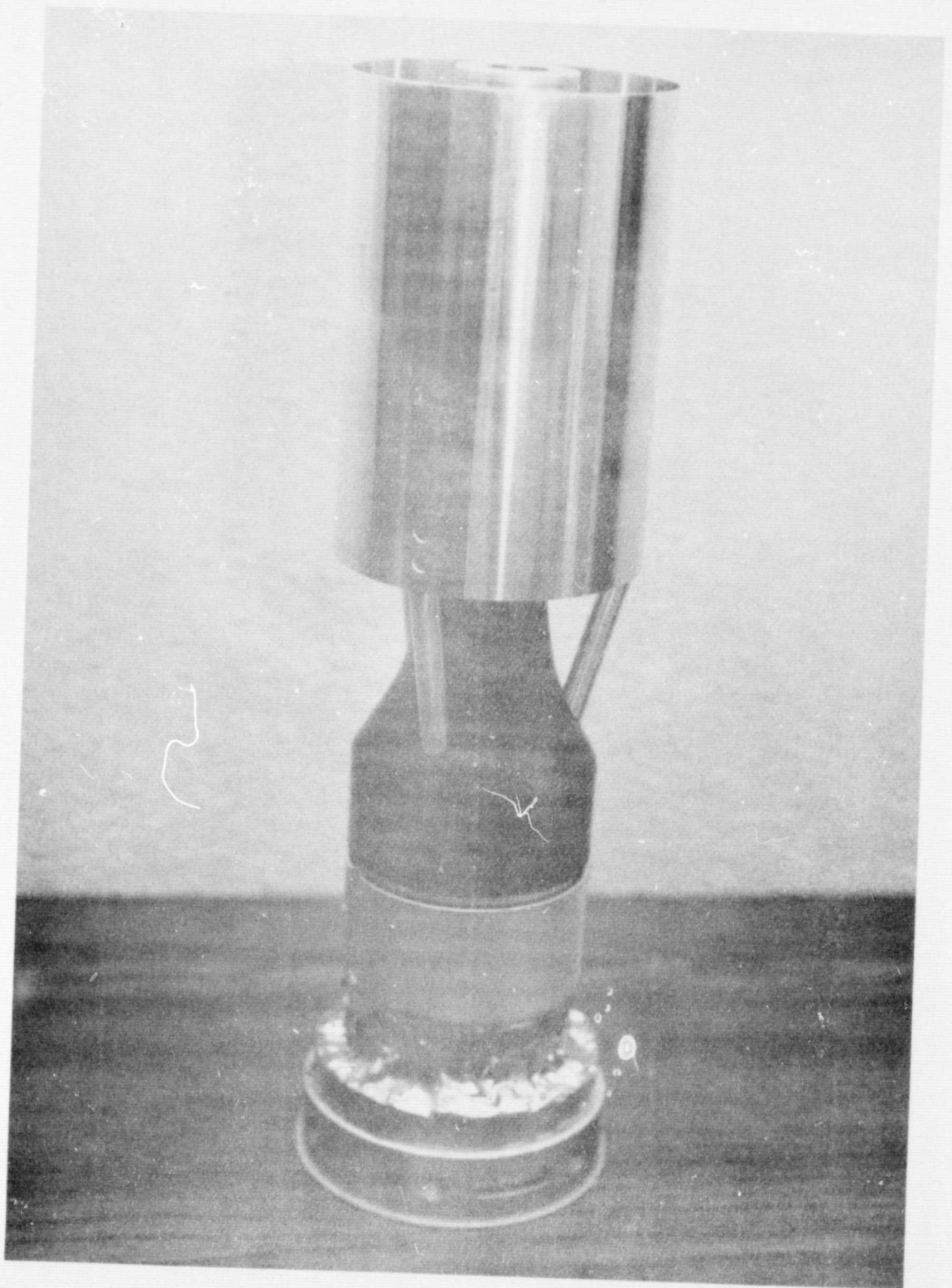


Figure 5.1: Gerdien condenser with flashing Lyman  $-\alpha$  lamp



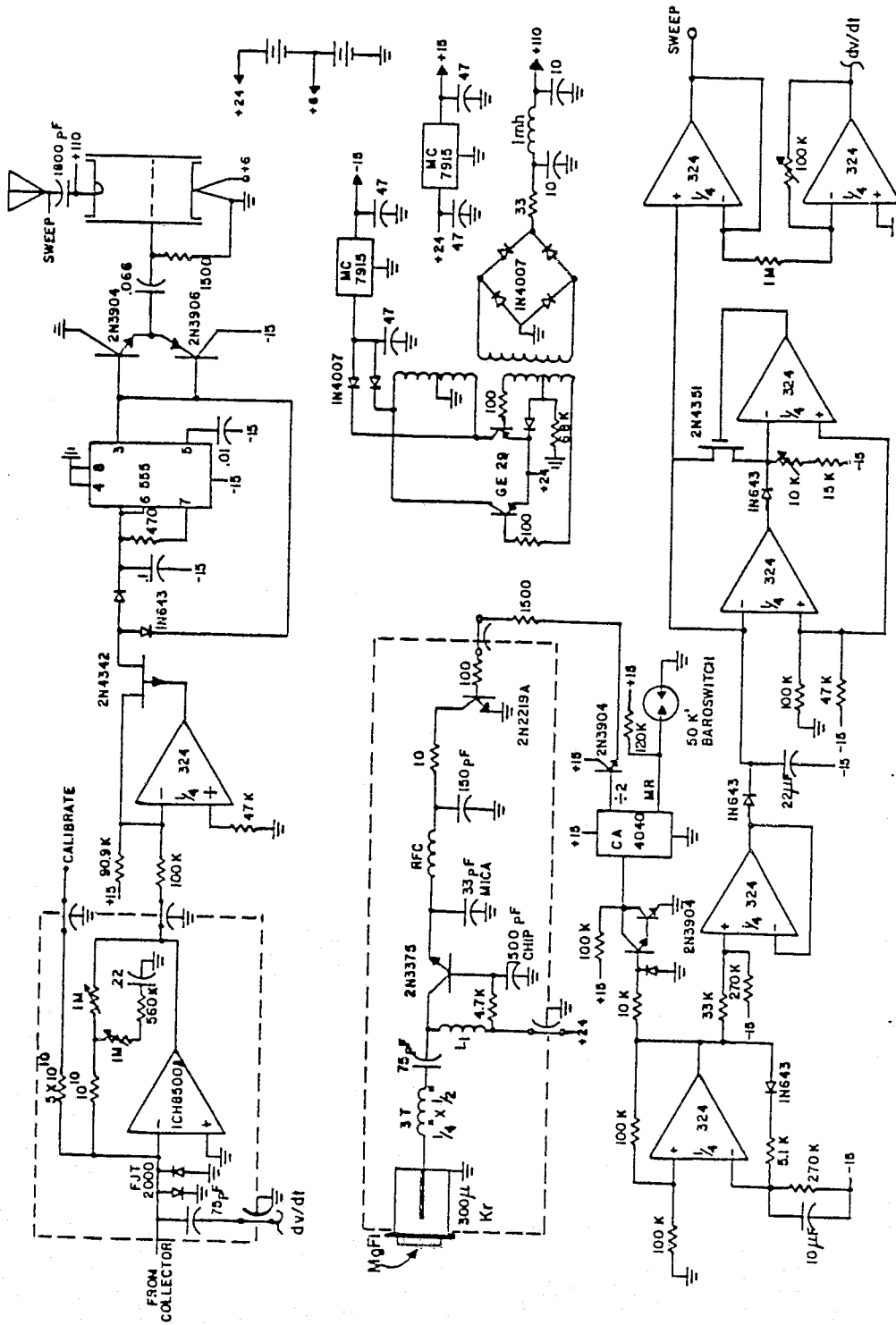


Figure 5.2: Gerdien condenser, Lyman- $\alpha$  probe schematic.

density non-rechargeable type. The chances of developing a reliable mechanical deployment of a Gerdien outer can for the Super Loki Dart also seem slim. The experiment itself is still undergoing evaluation; proper identification of the ion mobility types requires careful evaluation, and as experience is gained, the experiment parameters also evolve.

Considering the importance of a stable parachute to the Gerdien condenser and the increased complexity in reducing the data obtained, a synoptic system may be more useful as a blunt probe plus lamp configuration similar to that of Pontano and Hale (which may be feasible to incorporate in a Super Loki Dart). The larger Gerdien condensor probes would still be needed as diagnostic aids as to the ion products produced by the lamp.

CONCLUSION

A reduced cost conductivity probe system has been developed for synoptic studies. The existing Super Arcas blunt probe approach has been miniaturized for use with the 2-1/8 inch Super Loki Dart. A detailed assembly manual and blueprint have been generated to enable NASA in house as well as commercial production of these probes. Several developmental flights have been flown successfully and consultation support has been given to enable production of the probes in house at Wallops Flight Center. Development work has been done on an advanced probe which provides in situ ultraviolet-induced, additional ionization. While additional work needs to be done on this Lyman- $\alpha$  probe, the Super Loki blunt probe has proved itself to be a reliable experiment.

## REFERENCES

1. Hale, L. C., Space Research XIV (Akademie-Verlag, Berlin), 219, 1974.
2. Hale, L. C., D. P. Hoult, and D. C. Baker, Space Research VIII (North Holland, Amsterdam), 320, 1968.
3. Hoult, D. P., J. Geophys. Res., 70, 3183, 1965.
4. Sonin, A. A., J. Geophys. Res., 72, 4547, 1967.
5. Hale, L. C., Space Research VII (North Holland, Amsterdam), 140, 1967.
6. Mitchell, J. D., and L. C. Hale, Space Research XIII (Akademie-Verlag, Berlin), 471-476, 1973.
7. Cipriano, J. P., Scientific Report No. 410, Ionosphere Research Laboratory, The Pennsylvania State University, 1973.
8. Pontano, B. A., and L. C. Hale, Space Research X (North Holland, Amsterdam), 208, 1970.
9. Croskey, C. L., Scientific Report No. 442, Ionosphere Research Laboratory, The Pennsylvania State University, 1976.
10. Hale, L. C., C. L. Croskey and J. D. Mitchell, "Middle Atmosphere Ion Measurements During January, 1976," presented at COSPAR, June 1977, to be published in Space Research XVIII.
11. Hale, L. C. and D. P. Hoult, Scientific Report No. 247, Ionosphere Research Laboratory, The Pennsylvania State University, 1973.
12. Mitchell, J. D., Scientific Report No. 416, Ionosphere Research Laboratory, The Pennsylvania State University, 1973.
13. Hale, L. C., 1967, op. cit.
14. Mitchell, J. D., 1973, op. cit.
15. Georgian, E. J., and J. R. Griffin, Instrumentation Paper No. 174, Air Force Cambridge Research Laboratories, AFCRL-72-0089, 1977.
16. Pontano, B. A., and L. C. Hale, 1970, op. cit.